Article

Journal of
Nanoscience and Nanotechnology
Vol. 16, 2779–2782, 2016
www.aspbs.com/jnn

Nonlinear Transport in Organic Thin Film Transistors with Soluble Small Molecule Semiconductor

Hyeok Kim[1,†], Dong-Seok Song[2,†], Jin-Hyuk Kwon[2], Ji-Hoon Jung[2], Do-Kyung Kim[2], SeongMin Kim[3], In Man Kang[2], Jonghoo Park[4], Heung-Sik Tae[2], Nicolas Battaglini[5], Philippe Lang[5], Gilles Horowitz[6], and Jin-Hyuk Bae[2,*]

[1] *Construction Equipment Technology Center, Korea Institute of Industrial Technology (KITECH), Hayang-ro 13-13, Gyeongsan 38430, Korea*
[2] *School of Electronics Engineering, Kyungpook National University, Daegu 702-701, Korea*
[3] *Computational Science Group, Samsung Advanced Institute of Technology (SAIT), Yongin, Gyeonggi-do 446-712, Korea*
[4] *Department of Electrical Engineering, Kyungpook National University, Daegu 702-701, Korea*
[5] *ITODYS, CNRS UMR 7086, Université Paris Diderot (Paris7), 15 rue Jean-Antoine de Baïf, 75205 Paris Cedex 13, France*
[6] *LPICM, Ecole Polytechnique, CNRS, 91128 Palaiseau, France*

Nonlinear transport is intensively explained through Poole-Frenkel (PF) transport mechanism in organic thin film transistors with solution-processed small molecules, which is, 6,13-bis(triisopropylsilylethynyl) (TIPS) pentacene. We outline a detailed electrical study that identifies the source to drain field dependent mobility. Devices with diverse channel lengths enable the extensive exhibition of field dependent mobility due to thermal activation of carriers among traps.

Keywords: Nonlinear Transport, Poole-Frenkel Conduction, Organic Thin Film Transistors (OTFTs), 6,13-bis(triisopropylsilylethynyl) (TIPS) pentacene.

1. INTRODUCTION

Organic thin-film transistors (OTFTs) have attracted a lot of attention for several advantages such as the mechanical flexibility, the low-temperature processing capability with low cost, and the applicability to plastic substrates[1–4] over conventional silicon-based electronic elements since last several decades ago. In contrast to many of the OTFTs that experience generally from poor electrical properties, for instance, low current on–off ratio and low charge carrier mobility,[5–7] pentacene-based TFTs fabricated by vacuum-deposition have shown the prominent carrier mobility comparable to the level of amorphous silicon.[8–10]

In particular, solution-processed small molecules have huge potential in microelectronics applications by providing low cost processing and high charge carrier mobility. 6,13-bis(triisopropylsilylethynyl) (TIPS) pentacene has been widely used as an channel semiconductor boosting high performance thin film transistors with solution process.[11–14] Recently, TFT with TIPS pentacene appeared extremely high mobility due to its a number of novel processing technology. Shearing method using sliding plate induced directed crystal growth and it led high performance TFT with the mobility up to 4.6 cm^2/Vs through well-aligned crystals domains.[15] Advanced process based on the shearing method controlling fluid of semiconducting solution with micropillar-patterned blade at the bottom of sliding plate facilitated a high degree of morphological control of thin films and exhibited an unprecedented maximum mobility up to 11 cm^2/Vs.[16] However, via a simple spin-coating, the optimization of the type of solvents gave the mobility of 2.82 cm^2/Vs in a conventional process.[17] In general, The mobility ranging from 0.01 cm^2/Vs to 0.1 cm^2/Vs were achieved without any surface modifications of dielectric as reported in this article.[18] Here, we firstly report that nonlinear transport is observed in OTFTs with solution processed small molecule although polymer semiconductor is known for its nonlinear behavior of

*Author to whom correspondence should be addressed.
†These two authors contributed equally to this work.

mobility according to lateral field.[19, 20] This phenomenon is comprehensively demonstrated in terms of Poole- Frenkel transport.

2. EXPERIMENTAL DETAILS

A bottom gate, top contact pentacene TFT used in our study was shown in Figure 1. An indium–tin-oxide (ITO) layer on a glass substrate was used as a gate electrode. The ITO patterned substrate was cleaned with acetone, isopropyl alcohol, methyl alcohol, and de-ionized water sequentially. A gate insulator of poly(4-vinylphenol) (PVP)[21] mixed with a thermal cross-linking agent of methylated poly(melamine-co-formaldehyde) (MMF) in 125 wt% was prepared as described previously.[22] The PVP with MMF was dissolved in propylene glycol methyl ether acetate (PGMEA) in 10 wt% and then spin-coated on the ITO patterned substrate. The spin-coated PVP layer was baked at 100 C for 1 min to remove any residual PGMEA, and subsequently baked for 5 min at 200 C to promote thermal cross-linking in the PVP layer.[23]

The thickness and the capacitance per unit area of the cross-linked PVP layer were about 550 nm and 6.52 nF/cm^2, respectively. An active layer was produced from a solution of the TIPS pentacene in 1.0 wt% in 1,2-dicholorobenzene on the PVP insulator by drop-casting and cured at 60 °C for 1 min on a hotplate at ambient condition to evaporate the solvent. The thickness of deposited TIPS pentacene was 200 nm.[24]

Note that the PVP gate insulator is chemically inert against the solvent of the TIPS pentacene, 1,2-dicholorobenzene. The source and drain electrodes of Au were deposited on the TIPS pentacene film through a shadow mask at the deposition rate of 1 Å/s. The thickness of Au was 80 nm. The channel length (L) in our TIPS pentacene TFTs was varied as 50, 80, 120 μm while the channel width (W) was fixed to be 2 mm. The electrical performance of the TIPS pentacene TFTs was measured using a semiconductor parameter analyzer (HP4155A) at room temperature (RT) under ambient pressure.

3. RESULTS AND DISCUSSION

Output characteristics are inhibited in Figure 2. Devices with different channel lengths essentially define that the devices are under various lateral field at the same drain voltage. Higher drain current is taken when channel length is narrower and gate voltage is higher. This is simply shown in the following equation.

$$I_{\mathrm{Dsat}} = (1/2)\mu_{\mathrm{sat}}(W/L)C_i(V_{\mathrm{GS}} - V_T)^2 \quad (1)$$

From the equation above, the effective saturation mobility μ_{sat} is extracted by plotting and extracting the slope of the square root of the drain current as a function of V_{GS} in the transfer characteristics in Figure 3. W and L are width and length of channel, respectively. C_i is the capacitance per unit area of the gate and V_T is the threshold voltage. Mobility is given to 0.17 cm^2/Vs, 0.07 cm^2/Vs and 0.06 cm^2/Vs as the channel length varies from 50 to 120 μm. Clear difference in mobility is prominently acquired even at the same condition but channel length.

Diverse channel lengths induce different lateral field applying to each device at the same drain voltage. This can be quantified as the following equation known as Poole-Frenkel conduction.[25]

$$\mu(E) = \mu_0 * \exp(\gamma\sqrt{E}) \quad (2)$$

Field dependent mobility shows the effect of variable E-field on the mobility where μ_0 is the zero-field mobility and the field dependent factor γ. In the devices where the contact resistances do not play a dominant role, the channel length dependence of the saturation mobility can be demonstrated in terms of the commonly observed PF effect in organic semiconductors.[26]

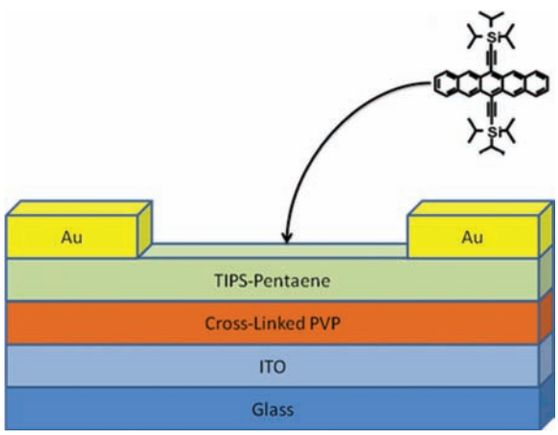

Figure 1. The schematic of a bottom gate, top contact TIPS pentacene TFT with a PVP gate insulator and the chemical structures of the TIPS pentacene.

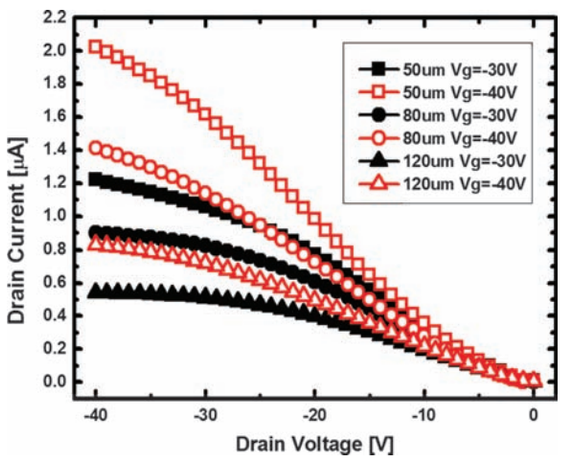

Figure 2. The output characteristics of three types of the TIPS pentacene TFTs.

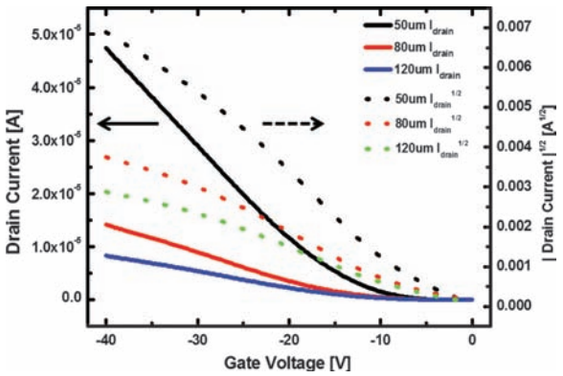

Figure 3. The transfer characteristics of three types of the TIPS pentacene TFTs.

For our analysis, we assumed that E is given by V_{DS}/L. Figure 4 exhibits a plot of saturation mobilities versus square root of E when V_{DS} is −40 V where the inset displays a log-linear plot of those for a set of the devices with channel length of 50, 80, 120 μm. The data for the three channel dominated devices fit reasonably well to the PF conduction model. From the slope of the fits, we extract the field dependent factor γ. At room temperature, γ deduced to 0.0016 cm^2/Vs which is reasonably at the general range of organic semiconductors.

The origin of the PF effect can be explained that the presence of disorder at the grain boundaries may be responsible for the lateral field dependence in the mobility. The strength of lateral field in the channel region should be high enough in order to provoke the PF effect in the transport. The electric field in the saturation regime is much higher than in the linear regime, thus, we measure saturation mobilities to find in more apparent regime.

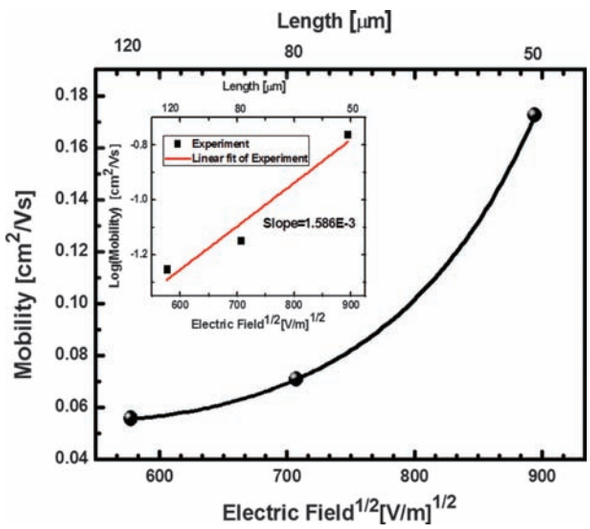

Figure 4. Saturation mobilities at $V_{DS} = -40$ V versus $E^{1/2}$ for the three types of the TIPS pentacene TFTs and inset shows log-linear plot to extrapolate a field dependent factor.

Enhanced charge injection may facilitate thetransport and higher mobility is induced at a higher lateral field.[27] Thus, the performance becomes contact limited for shorter channel length whilst suppressing the PF conduction in devices with higher contact resistance compared to channel resistance. However, we have used the high work function metal Au to guarantee low contact resistance to solution processed small molecular TFTs based on TIPS pentacene. Thus, PF conduction, which is originated from field-assisted hopping in trap states where are in energetic disorder or in defects of semiconductor, assists favorable charge transport through channel area.

4. CONCLUSION

Lateral field dependent mobility is found in solution processed small molecular TFTs. PF conduction mechanism is clearly suggested to explain the phenomenon. By taking advantage of the PF effect on the mobility in saturation, we acquired the mobility of up to 0.17 cm^2/Vs in solution processed small molecular TFTs with TIPS pentacene.

Acknowledgment: This work was supported by Basic Science Research Program through the National Research Foundation of Korea (NRF) funded by the Ministry of Education (2013R1A1A4A01009807).

References and Notes

1. C. D. Sheraw, L. Zhou, J. R. Huang, D. J. Gundlach, T. N. Jackson, M. G. Kane, I. G. Hill, M. S. Hammond, J. Campi, B. K. Greening, J. Franci, and J. L. West, *Appl. Phys. Lett.* 80, 1088 (**2002**).
2. S. R. Forrest, *Nature* 428, 911 (**2004**).
3. C. R. Kagan, D. B. Mitzi, and C. D. Dimitrakopoulos, *Science* 286, 945 (**1999**).
4. L. Zhou, A. Wanga, S. C. Wu, J. Sun, S. Park, and T. N. Jackson, *Appl. Phys. Lett.* 88, 083502 (**2006**).
5. J. H. Kwon, J. H. Seo, S. I. Shin, K. H. Kim, D. H. Choi, I. B. Kang, H. Kang, and B.-K. Ju, *IEEE Trans. Electron. Dev.* 55, 500 (**2008**).
6. S. K. Park, Y. H. Kim, J. I. Han, D. G. Moon, W. K. Kim, and M. G. Kwak, *Synthetic Metal* 139, 377 (**2003**).
7. J.-H. Bae, S.-D. Lee, J. S. Choi, and J. Park, *J. Nanosci. Nanotechno.* 12, 4388 (**2012**).
8. J. B. Koo, S. Y. Kang, I. K. You, and K. S. Suh, *Solid-State Electron.* 53, 621 (**2009**).
9. Y. Kato, S. Iba, R. Teramoto, T. Sekitani, T. Someya, H. Kawaguchi, and T. Sakurai, *Appl. Phys. Lett.* 84, 3789 (**2004**).
10. X. H. Zhang, B. Domercq, X. Wang, S. Yoo, T. Kondo, Z. L. Wang, and B. Kippelen, *Org. Electron.* 8, 718 (**2007**).
11. D. Gupta, N. Jeon, and S. Yoo, *Org. Electron.* 9, 1026 (**2008**).
12. S. K. Park, J. E. Anthony, D. A. Mourey, and T. N. Jackson, *Appl. Phys. Lett.* 91, 063514 (**2007**).
13. J. Chen, C. K. Tee, M. Shtein, D. C. Martin, and J. Anthony, *Org. Electron.* 10, 696 (**2009**).
14. J.-H. Kwon, S.-I. Shin, J. Choi, M.-H. Chung, T.-Y. Oh, K.-H. Kim, D. H. Choi, and B.-K. Ju, *J. Nanosci. Nanotechno.* 10, 3198 (**2010**).
15. G. Giri, E. Verploegen, S. C. B. Mannsfeld, S. Atahan-Evrenk, D. H. Kim, S. Y. Lee, H. A. Becerril, A. Aspuru-Guzik, M. F. Toney, and Z. Bao, *Nature* 480, 504 (**2011**).
16. Y. Diao, B. C. -K. Tee, G. Giri, J. Xu, D. H. Kim, H. A. Becerril, R. M. Stoltenberg, T. H. Lee, G. Xue, S. C. B. Mannsfeld, and Z. Bao, *Nat. Mater.* 12, 665 (**2013**).

17. D. K. Hwang, C. Fuentes-Hernandez, J. D. Berrigan, Y. Fang, J. Kim, W. J. Potscavage, Jr., H. Cheun, K. H. Sandhage, and B. Kippelen, *J. Mater. Chem.* 22, 5531 (**2012**).
18. B. Kang, W. H. Lee, and K. Cho, *ACS Appl. Mater. Interfaces* 5, 2302 (**2013**).
19. B. H. Hamadani and D. Natelson, *J. Appl. Phys.* 95, 1227 (**2004**).
20. B. H. Hamadani and D. J. Gundlach, *Appl. Phys. Lett.* 91, 243512 (**2007**).
21. H. Kim, J.-H. Bae, G. Horowitz, W. Y. Kim, and Y. Choi, *Solid-State Electron.* 81, 140 (**2013**).
22. H. Kim, J.-H. Bae, S.-D. Lee, and G. Horowitz, *Org. Electron.* 13, 1255 (**2012**).
23. J. H. Bae, J. Park, C. M. Keum, W. H. Kim, M. H. Kim, S. O. Kim, et al., *Org. Electron.* 11, 784 (**2010**).
24. J.-H. Bae, H. Kim, G. Horowitz, and S.-D. Lee, *Solid-State Electron.* 63, 163 (**2011**).
25. S. M. Sze, Physics of Semiconductor Devices, 2nd edn., Wiley, New York (**1981**).
26. H. Kim, G.-T. Park, Y. Nam, S. M. Kim, S. Kim, W.-Y. Lee, J.-H. Kwon, S. Park, C. Lee, J. Park, and J.-H. Bae, *Mol. Cryst. Liq Cryst.* 599, 79 (**2014**).
27. H. Kim, Z. Meihui, N. Battaglini, P. Lang, and G. Horowitz, *Org. Electron.* 14, 2108 (**2013**).

Received: 17 June 2014. Accepted: 25 December 2014.